Dynamic autonomous image segmentation based on Grow Cut

Alexandru Ion Marinescu[1,2], Zoltán Bálint[1,3], Laura Dioşan[1,2], Anca Andreica[1,2] *

1- IMOGEN Research Institute, County Clinical Emergency Hospital
400006, Cluj-Napoca, România

2- Faculty of Mathematics and Computer Sciences, Babeş-Bolyai University
400084, Cluj-Napoca, România

3- Faculty of Physics, Babeş-Bolyai University
400084, Cluj-Napoca, România

Abstract. The main incentive of this paper is to provide an enhanced approach for 2D medical image segmentation based on the Unsupervised Grow Cut algorithm, a method that requires no prior training. This paper assumes that the reader is, to some extent, familiar with cellular automata and their function as they make up the core of this technique. The benchmarks were performed on 2D MRI images of the heart and chest cavity. We obtained a significant increase in the output quality as compared to classical Unsupervised Grow Cut by using standard measures, based on the existence of accurate ground truth. This increase was obtained by dynamically altering the local threshold parameter. In conclusion, our approach provides the opportunity to become a building block of a computer aided diagnostic system.

1 Introduction

The medical context of the problem at hand is to quantify the degree of myocardium fibrosis located within the left atrium wall, with direct implications on deriving patient chances of recovery from persistent atrial fibrillation. From a technical standpoint, this relies on accurately segmenting the left atrium from the surrounding chest cavity and isolating it from the other 3 heart chambers. Ideally, this process should be unsupervised and fully automatic, yielding accurate results within a short time frame. To this end, we have analyzed state–of–the–art approaches and concluded that the most promising solution is the Unsupervised Grow Cut (UGC) [1] segmentation algorithm, since it is, foremost, autonomous, requiring minimal input from the end user (radiologist in our case). Moreover, it scales very well to highly parallel GPU architectures.

The plain-vanilla implementation of the UGC [1] suffers from a few drawbacks. Its threshold parameter, which governs the granularity of the segmentation, is not constant between different images, requiring manual adjustment. We propose two novel techniques which aim to overcome this caveat: *adaptive*

thresholding, in which the threshold is decreased with iteration count, and *priority thresholding*, in which unlabeled pixels from the original image are given higher priority over already labeled pixels.

The following sections first introduce the reader to a basic UGC algorithm and the way it functions, followed by our proposed approach and finally concluding with performance and preliminary numerical results.

2   Theoretical background

Image segmentation refers to the task of partitioning an image in sets of regions and therefore identifying objects of interest inside it. Existing techniques [2, 3] are still far from being able to fully automatically identify relevant features.

In this process we propose to make use of cellular automata (CAs) where, through appropriate choice of state transition rules and topologies, we can identify pixels which belong to the same cluster. In its most basic form, a CA is a triplet (S, N, ρ), with S being the set of states of each cell N, the cell's neighborhood and ρ is the state transition function which is applied with each iteration. The overall evolution of the CA's state has been shown to successfully model complex systems.

There are only few attempts in the literature to use CAs for image segmentation, but they confirm the scientific potential of the proposition [3, 4, 5]. One of the most popular approaches for image segmentation using cellular automata is given by the Grow Cut algorithm [6], which starts from several labeled seeds chosen by the user from the pixels of the image and automatically labels all the other pixels belonging to the image starting from the given seeds. A cellular automaton is used for propagating the labels of the seeds throughout the whole image.

There is, however, an autonomous method for CA based image segmentation which automatically generates random seed points and uses the Grow Cut algorithm for labeling, the so called Unsupervised Grow Cut (UGC) [1].

3   Proposed approach: adaptive and priority thresholding

The search for an optimal, fully–automatic segmentation algorithm has yet to yield a suitable result. Focusing on medical images, ideally such a segmentation procedure should meet the following criteria: fast execution time since the diagnostic process should not take more than a couple of minutes; low susceptibility to noise owing to the fact that MRI images, depending on the resolution of the scan and the capabilities of the acquisition device, contain various amounts of input noise; consistency of output, meaning that the results of the segmentation should be roughly the same if run multiple times on the same input image and finally high accuracy, approximating as close as possible the result from a radiologist's manual segmentation. Cellular automata are very well suited to parallelization on the CPU/GPU because in order to determine a cell's current

state all we need to know is its previous state and the state of all cells in its neighborhood.

Here we will detail our original contribution in the form of two variations of the UGC algorithm — adaptive and priority thresholding — followed by a hybrid approach these. The whole purpose of these techniques is to minimize noise and the number of unlabeled pixels while retaining region shape and size.

Adaptive Threshold — We thoroughly analyzed the evolution of the CA at each iteration and considered altering the threshold parameter with respect to the current iteration, aiming at first to obtain a rough segmentation of the image with clear distinction between different regions, and then as the iterations unfold, relax this threshold to merge small isolated pockets of regions, which are irrelevant to the desired output. We named this approach "adaptive thresholding" (and the resulting segmentation algorithm is called adaptive UGC). Apart from the threshold, number of iterations and neighborhood size parameters inherited from the UGC algorithm, we introduce two new parameters, namely $batchSize$ and $batchDecrement$, which operate on the threshold value in the following manner: after each $batchSize$ iterations, the threshold is decremented with $batchDecrement$. Please refer to section 4 for values of these parameters and their effect on the output.

Priority Threshold — Owing to the fact that the unlabeled pixels form a standalone category, we aimed to treat them differently from already labeled pixels during the CA update rule (priority UGC). Consider the following situations for two neighboring pixels P and Q (where Q belongs to the Moore neighborhood of P), where P is the current pixel in the center of the kernel and Q is a neighbor, trying to exert its influence upon P. If both P and Q are unlabeled, nothing happens in the current iteration. If both P and Q are labeled, compute the strength between P and Q and compare against $threshold$; if true, the label of P is equivalent to the label of Q. If P is unlabeled and Q is labeled, compute the strength between P and Q and compare against $threshold - tolerance$ (a small positive value, making it easier and faster for unlabeled pixels to acquire a label); if true, P takes the label of Q. By this mechanism we give unlabeled pixels priority in the labeling process over labeled ones. Finally, if P is labeled and Q is unlabeled nothing happens in the current iteration.

Hybrid Approach — Here we combine both adaptive and priority thresholding (hybrid UGC), benefits of which will be analyzed in the experimental results section. We can benefit simultaneously from both the threshold relaxing technique provided by the adaptive thresholding and the advantage in labeling black/unlabeled pixels from the priority thresholding. The order in which they are applied is as follows: first, if the current iteration is a multiple of $batchSize$, then the threshold is decremented by $batchDecrement$ units in order to favor labeling over fighting for pixels. Afterwards, during each iteration, we check whether the current pixel is unlabeled; if so, we give a higher priority over labeled ones for it, and as a consequence, making unlabeled/black pixels acquire a label earlier on.

4   Experimental results

We concentrated our efforts on the unsupervised version of the technique known in literature as the Grow Cut algorithm. In article [1], the authors process $64*64$ images for which 100 seeds are generated; by the rule of direct proportionality, in our $512*512$ images we should start with 6400 initial seeds, which are reduced at the end by equivalence to about 700 distinct classes.

The data we used for benchmarking, consisting of 2D MRI scans of the heart and chest cavity, have been acquired either with a 3T General Electric MRI scanner available at our IMOGEN Research Institute or via conversion from 3D Nifti format to a series of Dicom images, from the "MM-WHS 2017: Multi-Modality Whole Heart Segmentation" database [7, 8]. Out of the 20 MRI heart sequences available in this data set we have selected 10 images paired with existing ground truth elaborated by a trained radiologist, in the form of a binary labeled image – *true* for heart and *false* for surrounding tissue.

4.1   Performance measures

It is very important to establish the way we define similar regions or segments. The obtained segmentations and their boundaries could be compact, discontinuous, smooth etc. One of the metrics used in our experiments is the Dice coefficient, which computes the overlap between regions, quantifying the similarity of two segmentations. This measure is especially useful when the volume changes are of great importance in the analysis process. The Dice similarity coefficient [9] (denoted as DICE in this paper) is computed as the ratio between the number of pixels belonging to the intersection (of two possible segmentations) and the average of their sizes. Additionally, we also computed the classification accuracy (viewed as the distance between the real classifier and the modeled one) which is another important feature of a medical decision model [10].

4.2   Direct comparison

All experiments make use of the smallest, 3 by 3 Moore neighborhood. No post-processing or other techniques are involved unless specifically stated. Note, the color scheme of the labels has no medical meaning and is not related to the features of the pixels. It denotes only that two pixels of the same color belong to the same region.

Figure 1 contains visual segmentation results of the CA, run for 30 iterations, obtained by the plain-vanilla UGC (b), adaptive UGC with $batchSize$ 3 and $batchDecrement$ 0.001 (c), priority UGC, with $threshold - tolerance$ set to 0.05 (d) and hybrid UGC with the same parameters (e) for an MRI image of the heart and surrounding chest cavity (a) provided by the project's team of radiologists.

Table 1 contains the obtained numerical results for the 10 images (identified as 1001 to 1010) taken from [8]. Visceral segmentation evaluator [11] has been used for computing the following performance measures: Dice coefficient and accuracy. It can be observed that our proposed Adaptive UGC and, respectively,
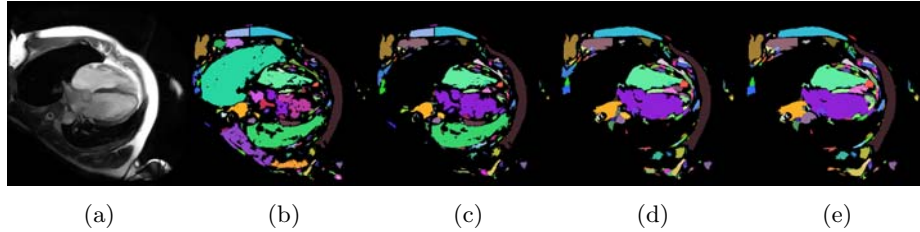
| (a) | (b) | (c) | (d) | (e) |

Fig. 1: (a) Example of an MRI image with the heart and chest cavity. (b) Plain-vanilla UGC. (c) Adaptive UGC. (d) Priority UGC. (e) Hybrid UGC.

ID	Dice			Accuracy		
	A%	**P%**	**H%**	**A%**	**P%**	**H%**
1001	16±0.02	17±0.02	34±0.04	1.6±0.01	-3.6±0.02	-0.4±0.02
1002	45±0.05	64±0.05	87±0.06	11.0±0.03	11.2±0.04	17.1±0.03
1003	27±0.03	59±0.03	80±0.03	3.4±0.01	4.2±0.02	7.1±0.01
1004	29±0.04	52±0.03	77±0.03	3.6±0.03	1.1±0.03	5.0±0.02
1005	35±0.03	70±0.03	94±0.03	3.0±0.01	1.8±0.01	3.5±0.01
1006	37±0.02	83±0.02	109±0.02	2.4±0.01	0.7±0.01	1.5±0.01
1007	32±0.03	58±0.02	79±0.03	4.3±0.01	5.3±0.01	8.4±0.01
1008	24±0.02	43±0.01	55±0.04	1.8±0.01	-1.7±0.01	-0.6±0.02
1009	24±0.05	30±0.05	42±0.04	4.5±0.02	4.4±0.02	6.7±0.01
1010	26±0.03	40±0.03	53±0.03	4.5±0.01	4.0±0.01	6.3±0.01

Table 1: Benchmark results showing percentage increase in quality over plain UGC. Due to the inherent nondeterministic property of the UGC algorithm, mean and standard deviation were extracted from a set of 30 trials per image. A% - adaptive UGC, P% - priority UGC, H% - hybrid UGC respectively (computed as $(UGCType - UGCPlain)/UGCPlain * 100$).

Priority UGC improve significantly over the classical UGC. Moreover, the hybrid approach combining Adaptive UGC and Priority UGC, provides even better results (Table 1).

Apart from a few cases, there can be noticed a significant increase in the accuracy and Dice coefficient when comparing to the ground truth image. The increase in quality is also observed as we progressively apply our adaptive and priority thresholding techniques, starting from plain-vanilla UGC, going through adaptive, priority and finally hybrid thresholding. The quality of the segmentation and fast execution time, in the order of a few seconds, owing to its OpenCL implementation, opens up an application possibility for other type of medical images.

5   Conclusions

In this work we present an improved version of the classical UGC algorithm that is well-suited to medical image segmentation. Our main contribution is an *adaptive thresholding* in which the threshold is decreased with iteration count, and a *priority thresholding*, in which unlabeled pixels from the original image are given higher priority over already labeled ones. We obtained a significant increase in the quality of the output by dynamically altering the local threshold parameter, which determines the granularity of the segmentation. Additionally, the method could be easily extended to 3D image segmentation task, requiring minimal adaptation of the parameters due to the increased number of interactions among neighboring voxels. Our approach, albeit it is still in research phase, could potentially be used as a building block of a computer-aided diagnostic (CAD) system.

References

[1] Payel Ghosh, Sameer K. Antani, L. Rodney Long, and George R. Thoma. Unsupervised grow-cut: Cellular automata-based medical image segmentation. In *Healthcare informatics, imaging and systems biology (HISB), 2011 first IEEE international conference on*, pages 40–47. IEEE, 2011.

[2] A. A. Abin, M. Fotouhi, and S. Kasaei. Cellular learning automata-based color image segmentation using adaptive chains. In *2009 14th International CSI Computer Conference*, pages 452–457, Oct 2009.

[3] Laura Dioşan, Anca Andreica, Imre Boros, and Irina Voiculescu. Avenues for the use of cellular automata in image segmentation. In Giovanni Squillero and Kevin Sim, editors, *Applications of Evolutionary Computation*, pages 282–296, Cham, 2017. Springer International Publishing.

[4] Yan Liu, Hengda Cheng, Jianhua Huang, Yingtao Zhang, and Xianglong Tang. An effective approach of lesion segmentation within the breast ultrasound image based on the cellular automata principle. *Journal of digital imaging*, 25(5):580–590, 2012.

[5] Blanca Priego, Daniel Souto, Francisco Bellas, and Richard J. Duro. Hyperspectral image segmentation through evolved cellular automata. *Pattern Recognition Letters*, 34(14):1648–1658, 2013.

[6] Vladimir Vezhnevets and Vadim Konouchine. Growcut - interactive multi-label n-d image segmentation by cellular automata. In *Russian Academy of Sciences*, pages 1–7. Russian Academy of Sciences, 2005.

[7] Xiahai Zhuang, Kawal S. Rhode, Reza S. Razavi, David J. Hawkes, and Sebastien Ourselin. A registration-based propagation framework for automatic whole heart segmentation of cardiac mri. *IEEE transactions on medical imaging*, 29(9):1612–1625, 2010.

[8] Xiahai Zhuang and Juan Shen. Multi-scale patch and multi-modality atlases for whole heart segmentation of mri. *Medical Image Analysis*, 31(1):77–87, 2016.

[9] Lee Raymond Dice. Measures of the amount of ecologic association between species. *Ecology*, 26(1):297–302, 1945.

[10] Fenster Aaron and Chiu Bernard. Evaluation of segmentation algorithms for medical imaging. In *Engineering in Medicine and Biology Society, 2005. IEEE-EMBS 2005. 27th Annual International Conference of the*, pages 7186–7189. IEEE, 2005.

[11] Oscar Alfonso Jiménez del Toro, Orcun Goksel, Bjoern Menze, Henning Müller, Georg Langs, Marc-André Weber, Ivan Eggel, Katharina Gruenberg, Markus Holzer, Georgios Kotsios-Kontokotsios, et al. Visceral–visual concept extraction challenge in radiology: Isbi 2014 challenge organization. Number 1194, pages 6–15, 2014.